mathematics

Article

High Steep Rock Slope Instability Mechanism Induced by the Pillar Deterioration in the Mountain Mining Area

Lu Chen [1], Xiangxi Yu [1], Ron Luo [2,3,*], Ling Zeng [1] and Hongtao Cao [1]

1 College of Civil Engineering, Changsha University of Science & Technology, Changsha 410110, China
2 School of Resource Environment and Safety Engineering, University of South China, Hengyang 421001, China
3 Periodical Press, Changsha University of Science & Technology, Changsha 410110, China
* Correspondence: luorong-lr@stu.usc.edu.cn

Abstract: In hilly regions, landslides or slope failures are very common phenomena, when underground mineral resources are excavated. In this study, some landslide disasters in a mountain mining area were analyzed. The engineering geological and instability reason were investigated. The numerical simulation of a high steep rock slope disturbed by a room and pillar mine was established. The failure process of a high steep rock slope induced by the pillar deterioration was analyzed to reveal the characteristics of deformation and sliding. The results show that the pillar plays an important role in maintaining the stability of the slope, if the pillar can support the overlying rock mass, only a tiny deformation will be induced. When the pillar fails and the roof caves, the overlying rock mass above the room and pillar goaf will rapidly subside, and the crack evolution of slope is induced, forming the potential slip surface. The landslide mass gradually moves. When the rock mass at the middle and lower of the slope is squeezed out, slope sliding will be induced. The failure process can be divided into four stages as follow: tiny displacement is caused by the mining, roof collapse is caused by the pillar failure, the potential slip surface is formed from the crack evolution; the slope sliding is induced by the fracturing of rock mass at the middle and lower of the slope.

Keywords: rock slope; goaf; pillar deterioration; crack evolution; slope instability

MSC: 65-04

check for updates

Citation: Chen, L.; Yu, X.; Luo, R.; Zeng, L.; Cao, H. High Steep Rock Slope Instability Mechanism Induced by the Pillar Deterioration in the Mountain Mining Area. *Mathematics* **2023**, *11*, 1889. https://doi.org/10.3390/math11081889

Academic Editor: José R. Fernánde

Received: 9 March 2023
Revised: 6 April 2023
Accepted: 12 April 2023
Published: 17 April 2023

1. Introduction

Mineral resources exploitation has made important contributions to the country's economic development in China. However, when resources are excavated in mountainous areas such as Guizhou and Guangxi Province, the subsidence and instability of overlying strata above the goaf can easily induce mountain cracking and landslide disasters, which seriously affect the safety of people's lives and property in the mountain mining areas [1–7]. Therefore, many scholars have investigated the influence of underground deposit mining on mountain stability. Fan, et al. [8] used field measurement, UAV aerial photography and remote sensing image methods to describe the characteristics of the collapse in the Pusa, a village in the County of Nayong (Guizhou Province, China), the dynamic process and formation mechanism of the collapse are then investigated. Dai et al. [9] analyzed the influence of underground mining disturbance on the deformation and failure of bedding rock slopes using a similar model test method. On this basis, the weakening phenomenon and weakening coefficient were defined, and the stability of the bedding rock slope affected by mining was studied by the limit equilibrium method. Salmi et al. [10] use the discrete element UDEC software to investigate the mechanism of mining-induced landsliding at NattaiNorth, NSW. The outcomes of numerical modeling showed that underground mining will cause the redistribution of stress within the rock mass, resulting in the weakening of the basement rock and the occurrence of shear failure. The failure of the collapsed bedrock of the overlying strata has been the main reason for large-scale landslides, and the instability mode is mainly controlled by the joints and fissures in the rock mass. Zhao et al. [11] studied the failure mechanism of the Madaling landslide 2006 in Guizhou Province, revealing that the slope experienced four stages of failure mechanisms, and the run-out behaviors of the landslide were analyzed. Zheng et al. [12] analyzed the failure process and mechanism associated with underground mining activities, based on field investigation and laboratory experimental study. The rockfalls are classified into one of three failure modes: crack–toppling, crack–sliding, and crack–slumping. In which the failures are governed by the corresponding characteristics of the rock mass structure. Zhong et al. [13] studied the formation mechanism of a slightly inclined bedding mudstone landslide in Tanshan Coal Mine in Ningxia by numerical simulation. It was found that the formation of the landslide is mainly affected by the geological factors of the mountain, coal mining and rainfall. The landslide process can be divided into four stages: slope creep, slope deformation, landslide movement and landslide accumulation. Yang et al. [14] simulated the deformation trend, mechanical behavior, fracture evolution process and deformation and failure mechanism of mining slope under different free surface characteristics by PFC 2D software. the deformation and failure process of the slope is divided into three stages: caving and sinking deformation stage-crack deformation stage-creep deformation stage. Zhang et al. [15] established a mining landslide sensitivity evaluation model based on transfer learning based on typical landslides, analyzing the main influencing factors of landslides in mining areas. Wang et al. [16] analyzed the behavior and characteristics of shallow failure of weak rock slopes through theoretical analysis, numerical simulation and field monitoring. It is found that the mechanical parameters of rock mass strength on the surface of weak rock slopes are quite different from those of the original rock after mining disturbance. The deformation of the lower part of the slope is three to five times that of the upper part, and its failure mode is creep crack.

The previous research shows that the instability and collapse of the slope is easily caused by the mining activity. Moreover, the outcomes have offered critical insight into the mechanism of the mining landslide [17–19]. However, researchers focus on the mechanical deformation characteristics and landslide formation mechanism, and the key role of the pillar in maintaining the stability of goaf is ignored. Some researchers have revealed that the collapse of goaf can be induced by the failure of the pillar [20–23]. To reveal the high steep rock slope instability mechanism induced by the pillar deterioration, some landslide disasters in mining areas were analyzed. Moreover, the numerical simulation of a high steep rock slope impacted by a room and pillar mine was established. The failure process of a rock high steep slope induced by the pillar deterioration was analyzed to reveal the characteristics of deformation and sliding.

2. Cases of High Steep Rock Slope Instability in Mining Area

2.1. Landslide in Pusa, Guizhou

2.1.1. Overview of Landslide

At about 10:40 on 28 August 2017, an extremely large landslide disaster occurred in the Laoyingyan Mountain in Pusa Village, Zhangjiawan Town, Nayong County, Guizhou Province as shown in Figure 1 [24]. The length of the landslide body was about 840 m, the width is about 410 m, and the landslide volume was about 6×105 m^3. It destroyed the local forest and cultivated land along the way and buried some houses in the Dashujiao Formation of Pusa Village, resulting in a total of 35 deaths [8].

Figure 1. Location of the slope instability [24].

2.1.2. Engineering Geological Condition

The collapse area was located in the upper part of the slope with a natural slope of 55~75°, and the lower part of the slope was a gentle slope with a slope of 10~25°. The dominant surrounding area was dry land. The exposed stratigraphic lithology includes as follows: limestone, silty mudstone and argillaceous siltstone in the Lower Triassic Yelang Formation(T1y); silty mudstone, limestone and argillaceous siltstone in the Upper Permian Changxing-Dalong Formation(P2c + d); the coal line of argillaceous siltstone, carbonaceous mudstone and coal seam in Longtan Formation (P2l). The lithology of the collapse area in Pusa Village is limestone, silty mudstone and argillaceous siltstone of the Lower Triassic Yelang Formation(T1y). The occurrence of the rock stratum is N80°E/SE∠5°~10°. The direction of the cliff wall is N40°~50° E, and the rock stratum is inclined to the slope [8]. The geological profile of the main sliding direction of the collapse in Nayong County, Guizhou Province is shown in Figure 2.

The collapsed area of the Pusa Village is characterized by a monoclinic structure. Moreover, the slope is constituted of a soft and hard interbedded structure rock mass. The limestone layer and marl layer are relatively hard. However, the argillaceous siltstone layer and silty mudstone layer are relatively weak. There are two faults (F1 and F2) in the mining area, which are located in the middle and front of the slope at the lower part of the cliff in the collapse source area. The coal seam in the mining area is fractured by those faults. However, the collapse source area is not impacted directly, as the dip direction of the fault is opposite to that of the rock stratum. Earthquake activity has not been found in this area and adjacent areas in recent years.

The lower part of the collapsed body is the mining area of the Pusa Coal Mine. Which mainly mines the coal seam of the Upper Permian Longtan Formation(P2l), the mind area is about 0.96 km^2. The dip angle of the mining coal seam is 7~12°. Among them, there are six coal seams, which are the M6, M10, M14, M16, M18 and M20 from top to bottom, with an average thickness of 1.6 m.

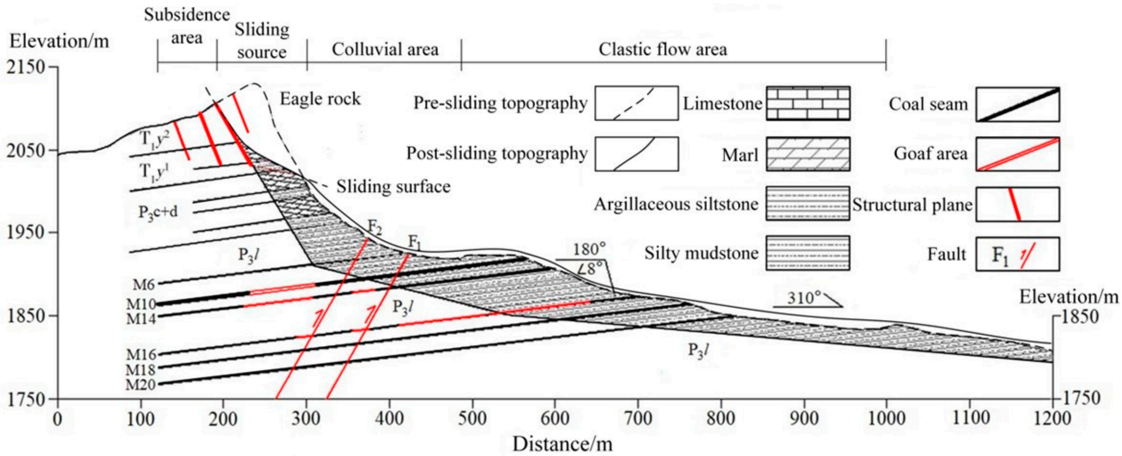

Figure 2. Geological profile of collapse at main sliding direction in Nayong County, Guizhou Province.

2.1.3. Instability Reason Speculation

The main factors causing landslide can be described as follows: the mining activities of the coal seam will affect and change the stress environment of the mountain, reducing the stability of the upper rock and soil. The structural plane, which is not conducive to the stability of rock mass, provides the natural conditions for mountain crack propagation. The dissolution and weathering of limestone rock mass accelerate the crack evolution, and the rainfall in the early stage deteriorates the geological conditions, as the strength of the rock will be weakened by the water [25,26].

2.2. Rockfall in the Kaiyang Phosphorite, Guizhou

2.2.1. Overview of Rockfall

The Kaiyang Phosphate Mine is located in Jinzhong, north of Guiyang, Guizhou Province as shown in Figure 1. According to the field investigation, a certain scale of collapse occurred frequently in the mining area. More than 80 times of collapses and landslides were induced with a total volume of more than 2.8 × 106 m^3. The geological section of the main sliding direction of a typical collapse in the Kaiyang Phosphate Mine is shown in Figure 3.

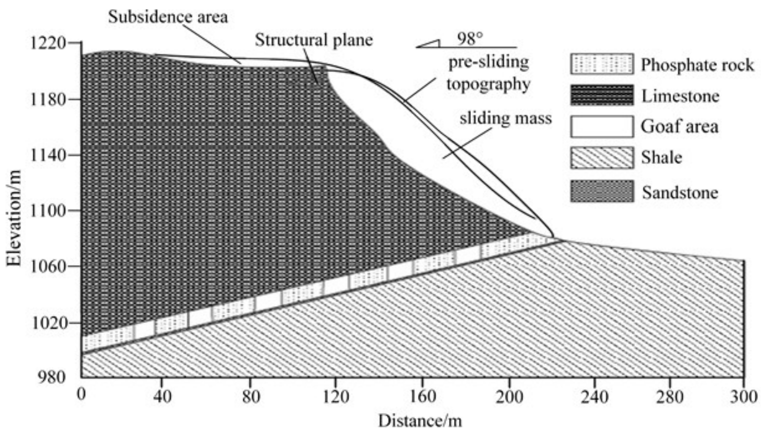

Figure 3. Geological Profile of Typical Collapse at Main Slip Direction in the Kaiyang Phosphate Mine.

2.2.2. Engineering Geological Condition

The terrain of the collapse area is high in the south and low in the north. The highest point of the Langjiling is 1203 m. The slope is steep, the gradient is 45~65°, and the occurrence of rock stratum is N13°E/SE∠30°. The strike of the slope is basically the same as that of the rock stratum, the direction of the dip is opposite, which belongs to the reverse layered structure slope [27].

The slope strata in the collapse area mainly include the Lower Cambrian Qingxudong Formation (ϵ1q) limestone, the Jindingshan Formation (ϵ1m) shale intercalated sandstone, the Mingxinsi Formation (ϵ1j) argillaceous sandstone, the Niutitang Formation (ϵ1n) carbonaceous shale, the Upper Sinian Dengying Formation (Zbdn) light gray thick dolomite, the Upper Sinian Doushantuo Formation (Zbd) phosphate rock and thin quartz sandstone and the Upper Sinian Nantuo Formation (Zann) purple red shale.

There are three groups of dominant structural planes in the collapse area. The structural plane J1 (N5°E/NW∠75°) constitutes the trailing edge boundary of the collapse area. The structural plane J2 (N15°E/NW∠47°) provides the bottom slip surface of the collapse. The structural plane J3 (N85°E/NW∠75°) is located downstream of the Yangshui River, which constitutes the lateral cutting surface of the collapse. Furthermore, unloading cracks inclined to the outside of the slope can be found in the slope.

2.2.3. Instability Reason Speculation

The long wall mining method is used in the rockfall area, and the regular pillars are retained to support the roof and stratum. The mining sequence is from top to bottom. A large mined-out area has been formed as long-term mining, and the overlying strata have been bent and sunk, inducing tensile cracks on the top and surface of the slope. As the steep and discussions of the slope, the potential sliding surface is easily caused. Furthermore, the rainfall is mainly concentrated from June to July. A large amount of rainwater infiltrates into the slope along the cracks on the top of the slope. While the rock mass is weakened, and the water pressure is produced. Those may induce to collapse of the slope in a critical state.

2.3. Weima Landslide, Shanxi

2.3.1. Overview of Landslide

On 16 August 2013, a landslide occurred at the crest of the Weima Mountain in Shanxi, China. The geological section of the main sliding direction is shown in Figure 4. The highest point elevation is 1471 m, the lowest point is located at the bottom of the slope, the elevation is 1436 m, the height difference is 35 m, and the landslide shear outlet elevation is 1437 m. The plane shape of the sliding body is an irregular oval. The length and width of the sliding body are about 62 m and 101 m, respectively, and the thickness is 5~13 m. The volume is about 5.6 × 104 m^3 which is considered a small bedrock landslide.

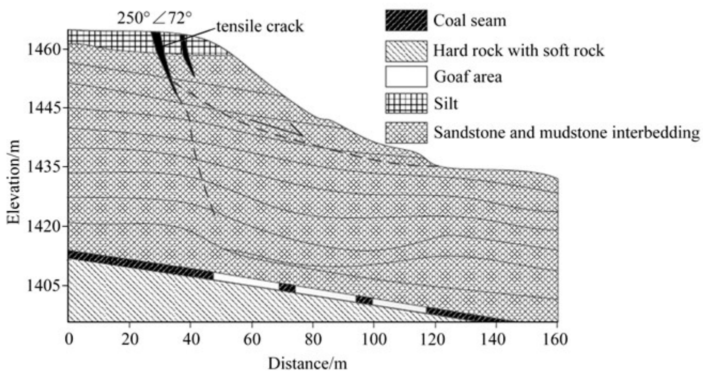

Figure 4. Geological Profile of landslide at Main Slide Direction in the Weima.

2.3.2. Engineering Geological Condition

The upper part of the slope in the landslide area is steep, with a slope angle of about 34°, and the lower part is gentle, with a slope of about 25°. The top layer of the slope is the quaternary silt with a thickness of about 3.15 m. The lower part of the slope is composed of sandstone, mudstone and coal. The occurrence of rock stratum is 165°∠10°, which is a bedding slope. Two groups of the 'X' type conjugate joints LX1 (330°∠80°) and LX2 (250°∠72°) are developed in the slope. The joint surface of LX1 is straight and smooth, and the joint surface of LX2 is serrated, with an opening width of 0.5–22.5 cm [28].

2.3.3. Instability Reason Speculation

The slope was disturbed by underground mining activity, and the underground coal mining in the landslide area can be traced back to the 1990s. The average thickness of the mined coal seam is 1.56 m, the buried depth is about 30~62 m, the short-wall blasting mining method is used, and the roof is managed by all caving methods. When the ore body is mined, a large area of goaf is formed, which causes the overlying rock mass to fall under the action of gravity, and the crack at the position of the trailing edge of the slope is induced as shown in Figure 1. Furthermore, the slope is also impacted by continuous heavy rainfall, the rainwater flows along the cracks, weakening the slope. Ultimately, the sliding is caused.

3. Numerical Simulation Analysis

3.1. Scheme of Numerical Simulation

In order to explore the instability mechanism of the high steep rock slope induced by the weakening of pillar in goaf, the PFC 2D (Particle Flow Code) discrete element software is used to study the mechanical behavior, revealing the dynamic instability mechanism of landslide in the mountain mining area. The length and width of the model are 450 m and 300 m, respectively. The thicknesses of limestone, marl, silty mudstone, coal seam, and argillaceous siltstone are 165 m, 15 m, 30 m, 9 m and 81 m, respectively. The parallel bond model is selected for coal and rock mass, the smooth joint model is selected for rock interface, and the Mohr–Coulomb criterion is used. The strength and deformation parameters in the numerical model (Tables 1 and 2) are determined by the previous research and rock mechanics test [29–33].

Table 1. Rock and coal parameters.

Parameters	Limestone	Marl	Silty Mudstone	Coal	Argillaceous Siltstone
Porosity/%	10	10	10	10	10
Particle density/(kg/m3)	2700	2650	2600	1350	2560
Effective modulus/GPa	10	8	7	3.84	5.6
Normal-to-shear stiffness ratio/k^*	1	1	1	1	1
Bond effective modulus/GPa	10	7	5	3.84	4.6
Bond normal-to-shear stiffness ratio/$\bar{k}^*$	1	1	1	1	1
Bond tensile strength/MPa	15	12.5	10.2	5.5	8
Bond cohesion/MPa	25	18.1	15.4	8	14.45
Bond friction angle/°	33	41	35.8	48	30.1

Table 2. Bedding planes parameters.

Parameters	Rock Interface	Coal Seam Interface
Bond effective modulus/GPa	2.9	1.5
Bond normal-to-shear stiffness ratio/($\bar{k}^*$)	1	1
Bond tensile strength/MPa	0.15	0.1
Bond cohesion/MPa	0.2	0.13
Bond friction angle/(°)	22	15

According to the engineering geological profile, a two-dimensional numerical model is established as shown in Figure 5. The horizontal displacement of the left and right boundaries is limited; the vertical displacement of the bottom boundary is also limited. The deformation and crack will be caused near the goaf first during the excavating, and the mining response propagates to the surface. The movement of the roof and overlying strata are monitored. In addition, this study focuses on the stability of the high and steep slope disturbed by mining activity, the deformation and crack evolution are analyzed, and the monitoring points at the top and the surface of the slope are arranged. Hence, twenty monitoring points are arranged at the top of the slope, the slope surface, the overlying rock mass and the roof of the goaf, those are divided into four groups as shown in Figure 5. The negative value of horizontal displacement indicates the monitoring point moves to the left of the mode, and the positive value of the horizontal displacement indicates that it moves to the right of the mode or the slope. The height of the mining is 5 m, and the spacing of the mining zone is 45 m. The mining sequence of the numerical model is from the M−1 to the M−3, and the calculation of stress balance is carried out after the mining of each working face.

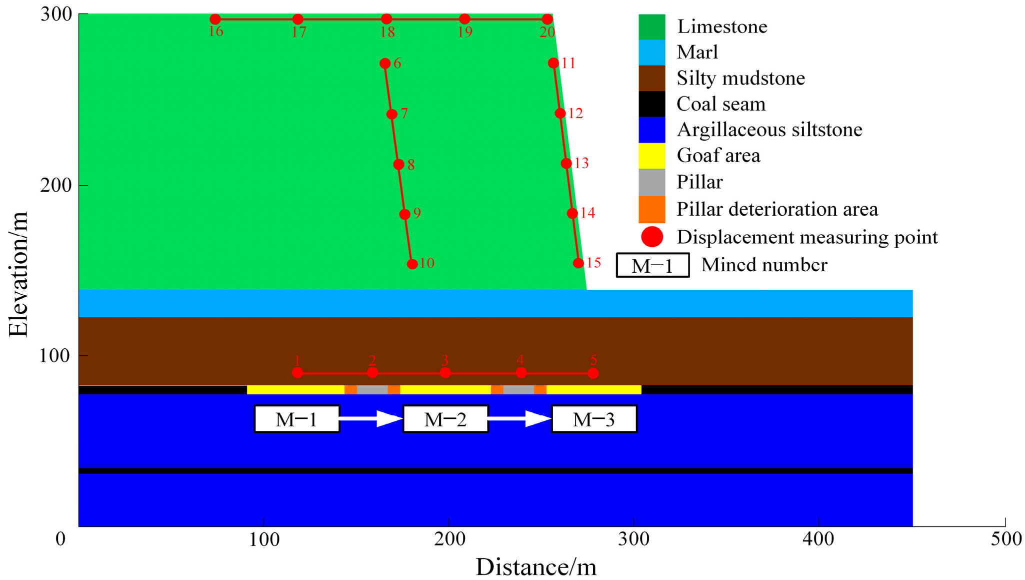

Figure 5. Numerical model and layout of monitoring points.

3.2. Analysis of the Failure Process

The process of cracking evolution and contact force characteristics of the numerical model are shown in Figure 6. When the coal seam is mined, the original stress state of the model is changed, which causes the stress redistribution of the surrounding rock, and the stress concentration occurs at the top of pillar and the boundary of the roof, resulting in cracks in the roof and the underlying weak rock mass as shown in Figure 6a. When the weakening pillar lost the bearing capacity, the roof deformation is caused due to the loss of support. Then, the roof sinks towards the goaf, and the shear crack of the roof is induced at the boundary of the goaf. When the stress of the roof strata in the goaf exceeds its ultimate bearing capacity, that will be gradually broken and then caved. In the process of roof caving, the overlying stratum also bends and sinks. Due to the roof caving, the subsidence of the overlying stratum is also caused, and a tensile fracture is formed inside the overlying rock mass as shown in Figure 6b. Then, the goaf is filled by the caved stratum, and the fracture and stress arch is formed in the slope. A collapse pit on the surface is formed at the top of the slope, accompanied by the visible deep cracks as shown in Figure 6c. When the pillar and roof collapse, the rock mass in the subsidence area is also broken due to the gravity of the overlying stratum. The uneven settlement continues to expand, resulting in the crack evolution of the slope. The slope body located at the right side of the macroscopic cracking dumps generally to the dip direction, and the rock mass at the foot of the slope is subjected to stress concentration due to the movement of the slope body as shown in

Figure 6d. With the continuous expansion of cracks, the potential sliding surface is formed in the slope. The rock mass at the middle and foot of the slope is continuously broken, and then squeezed out, the overburden slips downward due to the loss of support. The middle part of the slope is also cracked. With the continuous dumping of the slope, the sliding surface is penetrated, forming a potential landslide area. Ultimately, the sliding surface is connected, and a landslide is induced as shown in Figure 6e,f.

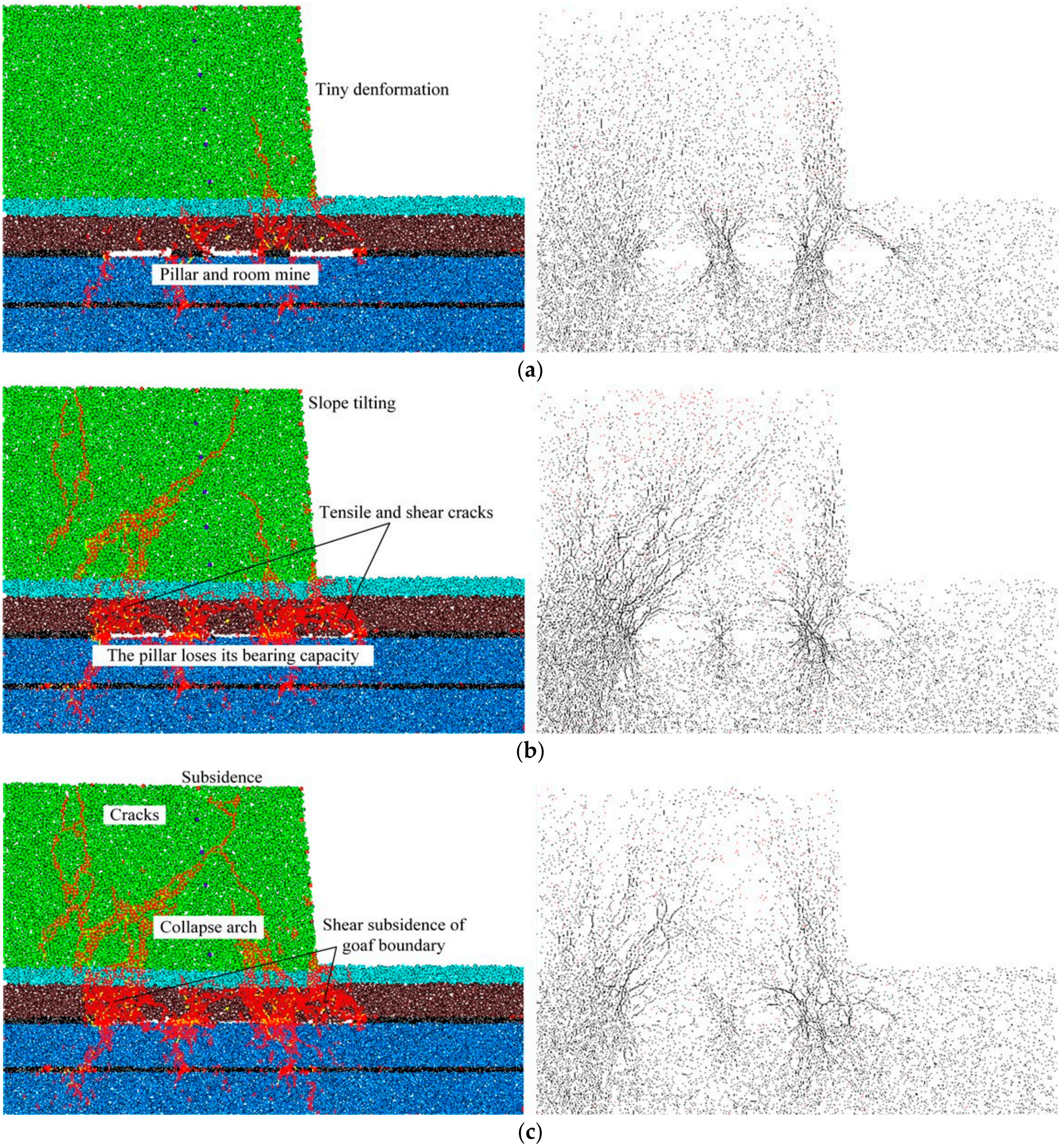

Figure 6. *Cont.*

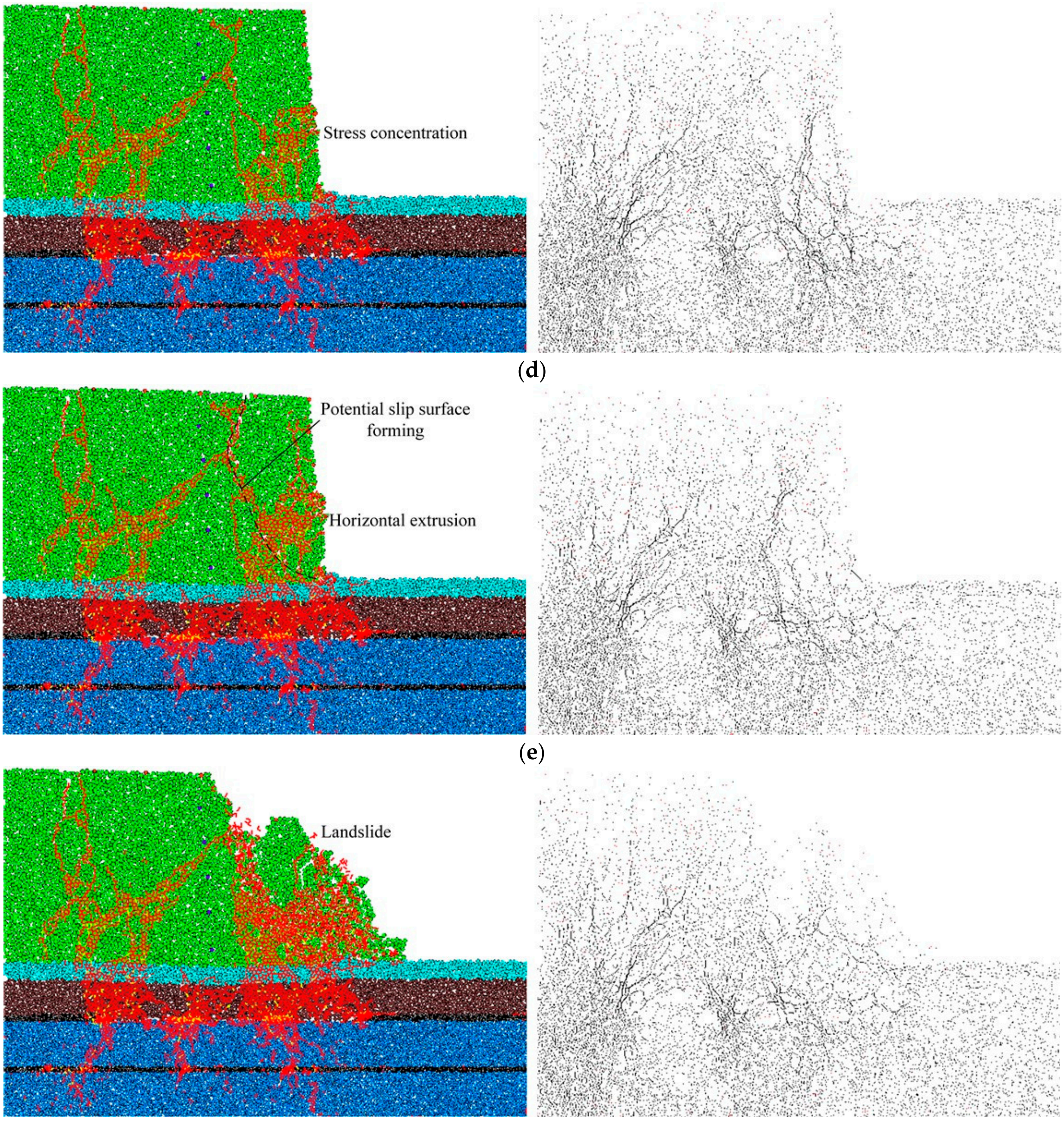

(**d**) (**e**) (**f**)

Figure 6. The process of cracking evolution and contact force characteristics. (**a**) mining; (**b**) pillar deterioration; (**c**) roof collapse and goaf filled; (**d**) rock mass spalling at slope; (**e**) potential slip surface forming; (**f**) landslide.

3.3. Analysis of Displacement Characteristics

The displacement laws of monitoring points arranged in roof are shown in Figure 7. When the areas of the M−1 and the M−2 are mined, a tiny displacement is induced. The downward deformation occurs firstly at the measuring point #1, followed by the #2 and #3. When the M−3 is mined, the negative displacement of the #1, #2 and #3 and the positive displacement of the #4 and #5 are induced. The vertical displacement of each measuring point in the roof maintains a small growth rate. Those indicate the measuring points of #1, #2 and #3 moved to the left of the model, and the measuring points of #4 and #5 moved to the right. The roof bends and sinks at the center of the goaf as a symmetrical point. Then, the vertical displacement of the roof increases sharply. Measuring point #5 moves fast to the slope. Both measuring points #3 and #4 move to the left first, and then to right. Those indicate the rapid subsidence of the roof has been induced by the degradation of the pillar. During the rapid subsidence process, the overlying strata are also toppling outward to the slope. Until the roof collapses and the overlying rock mass fills the goaf, the displacement of the measuring point stop growth.

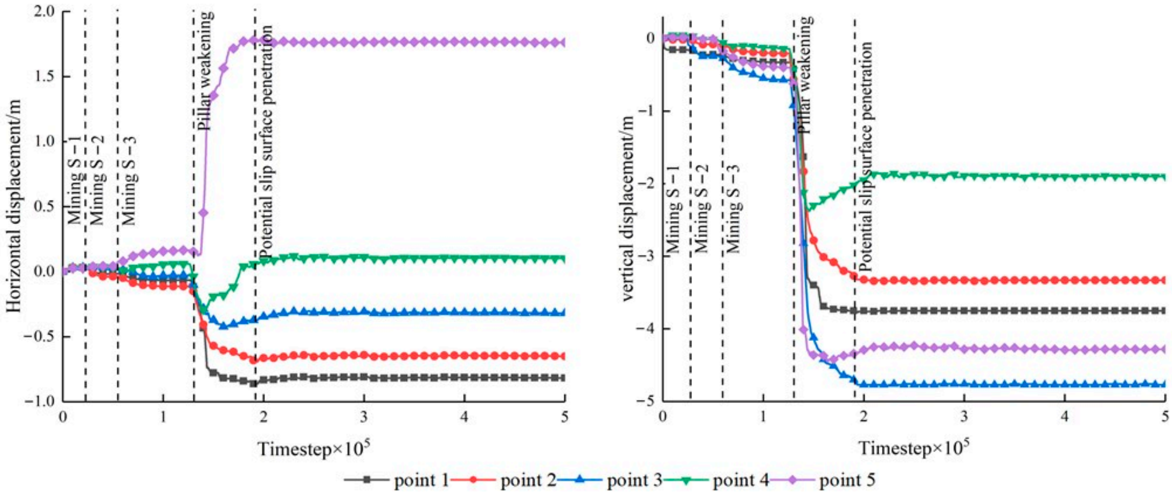

Figure 7. The displacement of the roof of pillar and room goaf.

The displacement laws of the measuring points above the M−2 are shown in Figure 8. It can be found that the tiny vertical displacement is caused by the mining activity, while the pillar has enough bearing capacity to support the overlying rock mass. However, the displacement of each measuring point changes greatly resulting from the deterioration of the pillar. The horizontal displacement develops positively, and the vertical displacement increases negatively. This indicates the rock mass above the M−2 moves to the slope and the goaf when the pillar lost its bearing capacity and the roof collapses. As the rock mass fills the goaf, the displacement of the measuring points also stops growth, indicating that the overlying strata above the M−2 keep stable after the subsidence.

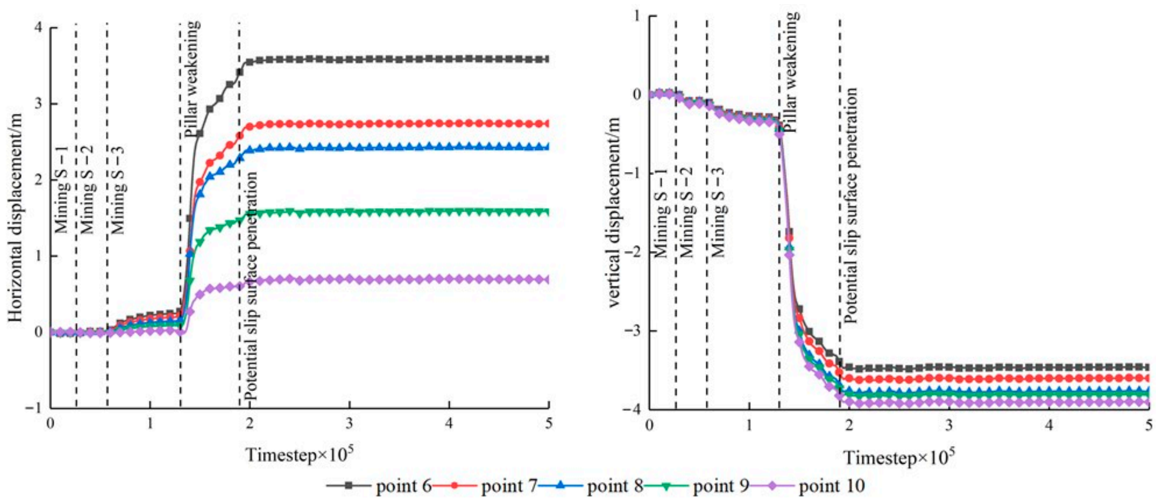

Figure 8. The displacement of strata above the M-2.

The horizontal and vertical displacement at the surface of slope are shown in Figure 9. A tiny displacement is caused during the mining process of the M−1, M−2 and M−3. However, a significant change appears after the pillar deterioration. The horizontal and vertical displacements increase rapidly at the same time, indicating the slope body tends to move to the dip direction of the slope. The horizontal displacement of measuring points #13 and #14 changed earlier than other measuring points. Those show that the rock mass in the middle and lower part of the slope is squeezed out firstly during the settlement deformation of the strata. As the distance between measuring point #15 and the bottom of the slope is small, the displacement value changes little during the process of slope instability. Moreover, the displacement stops changing when that rolls to the bottom of the slope.

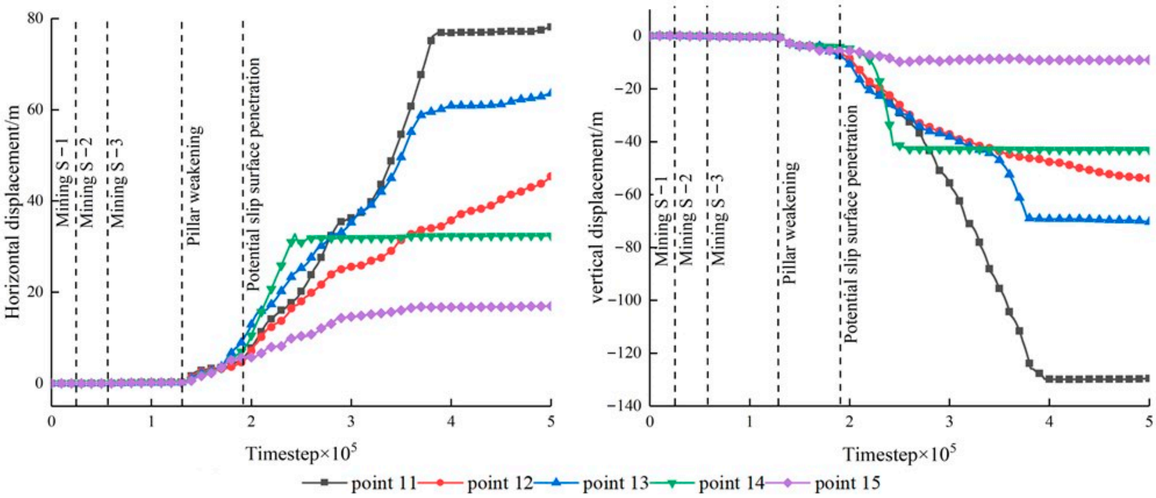

Figure 9. The displacement at the surface of slope.

The horizontal and vertical displacement at the top of the slope is shown in Figure 10. The displacement almost cannot be induced at the top of the slope during the mining process of the M−1, M−2 and M−3. When the bearing capacity of the pillar decreases, some measuring points start moving. The measuring points #16, #17 and #18 moved to the slope, caused by the deterioration of the pillar, and then stopped moving. However, measuring points #19 and #20 speedily moved again at the 1.1 $\times$ 10^5 timestep. Those indicate the slipping has been caused at the monitoring area of points #19 and #20. Moreover, the potential slip surface is located between monitoring points #18 and #19.

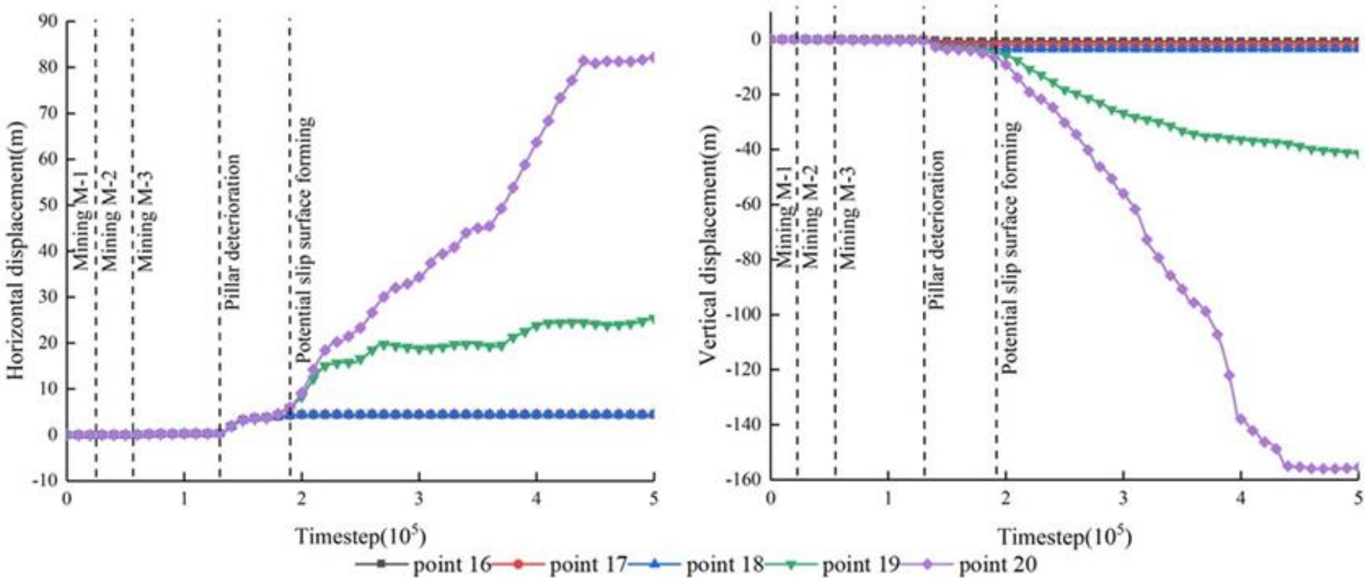

Figure 10. The displacement at the top of slope.

4. Slope Instability Mechanism Induced by the Pillar Deterioration

The failure process of landslide is shown in Figure 11. When the pillar and room goaf is formed, the stress of slope body is redistributed. Moreover, stress concentration occurs, resulting in the cracks evolution of rock mass in the slope. Before the pillar lost its bearing capacity, a tiny displacement is induced. However, when the pillar fails to bear the weight of the overlying rock mass, it causes subsidence in the roof. Moreover, the shear dislocation subsidence occurs at the goaf boundary near the slope toe. As the roof caves gradually, the tensile shear cracks at the boundary gradually expand upward, forming a collapsed arch. The overlying rock mass inclines outward to the dip direction of the slope with the collapsing of the goaf. Moreover, the serious stress concentration occurs at the rock mass in the middle and lower part of the slope. That rock mass is firstly destabilized and squeezed out. As a result, the overlying rock layer loses its support and also dumps outward. In this process, the overlying rock mass gradually breaks and forms the potential sliding surface, and finally slides out on the outside of the slope. Therefore, the instability mechanism of rock slope induced by the pillar deterioration can be summarized as follows:

(I) Tiny displacement is caused by the mining (Figure 11a).
(II) Roof collapse is caused by pillar failure (Figure 11b).
(III) Macro-crack of the slope is induced by the overburdened rock movement, forming the potential slip surface (Figure 11c).
(VI) The rock mass at the middle and lower of the slope is squeezed out, inducing the slope sliding (Figure 11d).

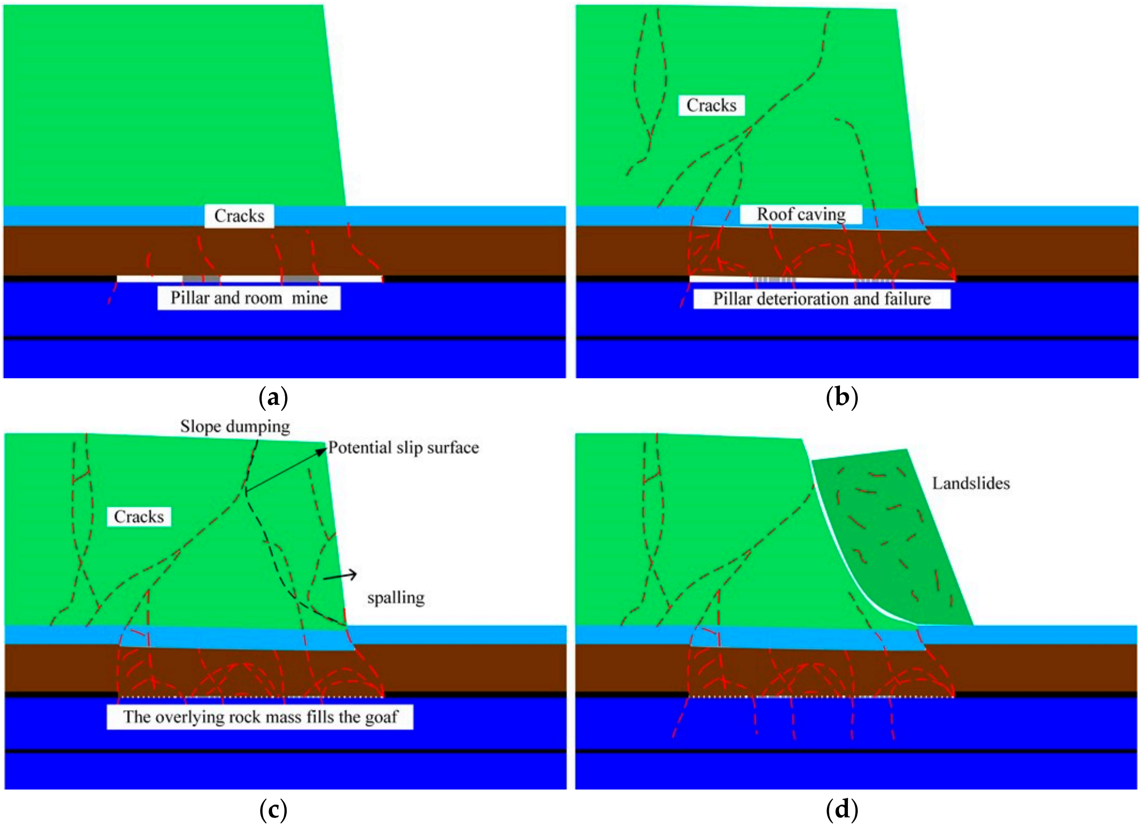

Figure 11. Failure process. (**a**) mining; (**b**) pillar deterioration; (**c**) potential slip surface forming; (**d**) landslide.

5. Discussion and Conclusions

(1) The stability of high steep rock slope is significantly disturbed by mining activity. Especially, the crack and the overall deformation of the slope will be caused by the failure of pillar. When the overburden rock subsides and the slope gradually topples to dip the

direction of the slope. The stability of the slope is greatly affected. The slope sliding is easily induced by the changing external environment conditions.

(2) The pillar may play an important role in process of the deformation and failure of the slope. When the mined-out area is formed, if the pillar can bear the weight of the overlying rock mass, only a tiny deformation can be induced. The impact of slope stability disturbed by mining will be restricted, and the slope will form a new stable state. With the passing of time, if the bearing capacity of the pillar is reduced due to the spalling and strength deterioration, when the pillar is destroyed, the overlying rock mass above the goaf will rapidly subside, which is considered to be responsible for the deformation and instability of the slope.

(3) The failure process of rock slope induced by pillar degradation in goaf can be divided into four stages in this study. (I) Tiny displacement is caused by mining. (II) Roof collapse is caused by pillar failure. (III) The potential slip surface formed results from the crack evolution. (IV) The slope sliding is induced by the fracturing of rock mass at the middle and lower of the slope.

Author Contributions: Conceptualization, L.C.; Data curation, X.Y.; Formal analysis, R.L.; Funding acquisition, L.C.; Investigation, R.L.; Methodology, X.Y.; Project administration, X.Y.; Resources, X.Y. and H.C.; Software, X.Y. and H.C.; Supervision, L.C. and L.Z.; Validation, L.C. and L.Z.; Visualization, R.L.; Writing—original draft, X.Y. All authors have read and agreed to the published version of the manuscript.

Funding: This research was funded by the National Natural Science Foundation of China (52004036, 52078066 and 52078067); the National Natural Science Foundation of Hunan Province (2021JJ40572 and 2021JJ40579), and the Postgraduate Scientific Research Innovation Project of Changsha University of Science & Technology (CX2021SS23).

Data Availability Statement: Data sharing not applicable. The data and materials are contained within the article.

Acknowledgments: We would like to acknowledge the editors and reviewers for their invaluable comments.

Conflicts of Interest: The authors declare no conflict of interest.

References

1. Yu, X.; Mao, X. A preliminary discrimination model of a deep mining landslide and its application in the Guanwen coal mine. *Bull. Eng. Geol. Environ.* **2020**, *79*, 485–493.
2. Yang, Y.; Xu, Y.; Shen, S.; Yuan, Y.; Yin, Z. Mining-induced geo-hazards with environmental protection measures in Yunnan, China: An overview. *Bull. Eng. Geol. Environ.* **2015**, *74*, 141–150. [CrossRef]
3. Zhong, Z.; Xu, Y.; Wang, N.; Liu, X.; Gao, G. Environmental characteristics and unified failure mode classification system for mining landslides in the karst mountainous areas of southwestern China. *Carbonates Evaporites* **2023**, *38*, 2. [CrossRef]
4. Chen, L.; Zhao, C.; Li, B.; He, K.; Ren, C.; Liu, X.; Liu, D. Deformation monitoring and failure mode research of mining-induced jianshanying landslide in karst mountain area, China with ALOS/PALSAR-2 images. *Landslides* **2021**, *18*, 2739–2750. [CrossRef]
5. Cheng, X.; Qi, W.; Huang, Q.; Zhao, X.; Fang, R.; Xu, J. Typical geo-hazards and countermeasures of mines in Yunnan province, southwest China. *IOP Conf. Ser. Earth Environ. Sci.* **2016**, *44*, 022008. [CrossRef]
6. Tong, L.; Liu, L.; Yu, Q. Highway construction across heavily mined ground and steep topography in southern China. *Bull. Eng. Geol. Environ.* **2014**, *73*, 43–60. [CrossRef]
7. Xiao, J. Analysis of the main causes of a composite landslide in Guizhou province. *J. Transp. Sci. Eng.* **2020**, *36*, 40–44. (In Chinese)
8. Fan, X.; Xu, Q.; Scaringi, G.; Zheng, G.; Huang, R.; Dai, L.; Ju, Y. The "long" runout rock avalanche in Pusa, China, on august 28, 2017: A preliminary report. *Landslides* **2019**, *16*, 139–154. [CrossRef]
9. Dai, Z.; Zhang, L.; Wang, Y.; Jiang, Z.; Xu, S. Deformation and failure response characteristics and stability analysis of bedding rock slope after underground adverse slope mining. *Bull. Eng. Geol. Environ.* **2021**, *80*, 4405–4422. [CrossRef]
10. Salmi, E.; Nazem, M.; Karakus, M. Numerical analysis of a large landslide induced by coal mining subsidence. *Eng. Geology.* **2017**, *217*, 141–152. [CrossRef]
11. Zhao, J.; Xiao, J.; Lee, M.; Ma, Y. Discrete element modeling of a mining-induced rock slide. *Springer Plus* **2016**, *5*, 1633. [CrossRef] [PubMed]
12. Zheng, D.; Frost, J.D.; Huang, R.Q.; Liu, F.Z. Failure process and modes of rockfall induced by underground mining: A case study of Kaiyang phosphorite mine rockfalls. *Eng. Geol.* **2015**, *197*, 145–157. [CrossRef]

13. Zhong, J.; Mao, Z.; Ni, W.; Zhang, J.; Liu, G.; Zhang, J.; Geng, M. Analysis of formation mechanism of slightly inclined bedding mudstone landslide in coal mining subsidence area based on finite–discrete element method. *Mathematics* **2022**, *10*, 3995. [CrossRef]
14. Yang, C.; Shi, W.; Peng, X.; Zhang, S.; Wang, X. Numerical simulation of layered anti-inclined mining slopes based on different free face characteristics. *Bull. Eng. Geol. Environ.* **2022**, *81*, 359. [CrossRef]
15. Zhang, Y.; Yang, Y.; Zhang, J.; Wang, Y. Sensitivity study of multi-field information maps of typical landslides in mining areas based on transfer learning. *Front. Earth Sci.* **2023**, *11*, 1105985. [CrossRef]
16. Wang, W.; Yan, Y.; Qu, Y.; Wang, P. Shallow failure of weak slopes in Bayan Obo west mine. *Int. J. Environ. Res. Public Health.* **2022**, *19*, 9755. [CrossRef]
17. Nie, L.; Li, Z.; Zhang, M.; Xu, L. Deformation characteristics and mechanism of the landslide in west open-pit mine, Fushun, China. *Arab. J. Geosci.* **2015**, *8*, 4457–4468. [CrossRef]
18. Li, J.; Li, B.; He, K.; Gao, Y.; Wan, J.; Wu, W.; Zhang, H. Failure mechanism analysis of mining-induced landslide based on geophysical investigation and numerical modelling using distinct element method. *Remote Sens.* **2022**, *14*, 6071. [CrossRef]
19. Li, J.; Li, B.; Gao, Y.; Cui, F.; He, K.; Li, J.; Li, H. Mechanism of overlying strata migration and failure during underground mining in the mountainous carbonate areas in southwestern China. *Front. Earth Sci.* **2022**, *10*, 498. [CrossRef]
20. Cao, Z.; Zhou, Y. Research on coal pillar width in roadway driving along goaf based on the stability of key block. *CMC-Comput. Mater. Contin.* **2015**, *48*, 77–90.
21. Guo, J.; Cheng, X.; Lu, J.; Zhao, Y.; Xie, X. Research on factors affecting mine wall stability in isolated pillar mining in deep mines. *Minerals* **2022**, *12*, 623. [CrossRef]
22. Reed, G.; Mctyer, K.; Frith, R. An assessment of coal pillar system stability criteria based on a mechanistic evaluation of the interaction between coal pillars and the overburden. *Int. J. Min. Sci. Technol.* **2017**, *27*, 9–15. [CrossRef]
23. Zhou, Z.; Cai, X.; Li, X.; Cao, W.; Du, X. Dynamic response and energy evolution of sandstone under coupled static–dynamic compression: Insights from experimental study into deep rock engineering applications. *Rock Mech. Rock Eng.* **2020**, *53*, 1305–1331. [CrossRef]
24. China Geological Survey. Topographic Map of Guizhou Province. (2018-10-31). Available online: https://geocloudproducts.cgs.gov.cn/dzzlfw/idx/fileView.do?dzcp_id=d9b9919f3f0b4d709b073fb85ae37188&path=https%3A%2F%2Fgeocloudproducts.cgs.gov.cn%2Fdzxxcp%2Fadmin_file%2Fcore%2Ffile%2FtoView.do%3Fid%3Df6852a644b6a4d3aa06c1036e9db5f1a%26t%3Ddeepzoom&providerid=4028803a518fe41c0151a47891240027 (accessed on 31 March 2023).
25. Cai, X.; Zhou, Z.; Zang, H.; Song, Z. Water saturation effects on dynamic behavior and microstructure damage of sandstone: Phenomena and mechanisms. *Eng. Geol.* **2020**, *276*, 105760. [CrossRef]
26. Fu, Y.; Liu, Z.; Zeng, L.; Gao, Q.; Luo, J.; Xiao, X. Numerical analysis method that considers weathering and water-softening effects for the slope stability of carbonaceous mudstone. *Int. J. Environ. Res. Public Health.* **2022**, *19*, 14308. [CrossRef] [PubMed]
27. Huang, G.; Zheng, D. The formation mechanism and numerical simulation of the collapse of Kaiyang phosphate mine in Guizhou. *Chin. J. Geol. Hazard Control.* **2013**, *24*, 46–50+55. (In Chinese)
28. Duan, P. Analysis on the formation mechanism of overlying landslide in goaf. *Min. Technol.* **2019**, *19*, 68–71. (In Chinese)
29. Zhou, Z.; Chen, L.; Zhao, Y.; Zhao, T.; Cai, X.; Du, X. Experimental and numerical investigation on the bearing and failure mechanism of multiple pillars under overburden. *Rock Mech. Rock Eng.* **2017**, *50*, 995–1010. [CrossRef]
30. Zhou, Z.; Zhao, Y.; Cao, W.; Chen, L.; Zhou, J. Dynamic response of pillar workings induced by sudden pillar recovery. *Rock Mech. Rock Eng.* **2018**, *51*, 3075–3090. [CrossRef]
31. Qiu, Y.; Shang, Y. Analysis of progressive failure mechanism of loose slope under seismic load. *J. China Foreign Highw.* **2022**, *42*, 15–21. (In Chinese)
32. Zhao, Q.; Yang, Z.; Jiang, Y.; Liu, X.; Cui, F.; Li, B. Discrete element analysis of deformation features of slope controlled by karst fissures under the mining effect: A case study of Pusa landslide, China. *Geomat. Nat. Hazards Risk* **2023**, *14*, 1–35. [CrossRef]
33. Wang, N.; Zhong, Z.; Liu, X.; Gao, G. Failure mechanism of anti-inclined karst slope induced by underground multiseam mining. *Geofluids* **2022**, *2022*, 1302861. [CrossRef]